

RESEARCH ARTICLE

Protein tyrosine phosphatase PTPN9 regulates erythroid cell development through STAT3 dephosphorylation in zebrafish

Ye Bu¹, Fuqin Su², Xu Wang¹, Hai Gao^{1,3}, Lei Lei¹, Nannan Chang¹, Qing Wu¹, Keping Hu³, Xiaojun Zhu¹, Zhijie Chang², Kun Meng^{4,*} and Jing-Wei Xiong^{1,*}

ABSTRACT

Protein tyrosine phosphatases (PTPs) are involved in hematopoiesis, but the function of many PTPs is not well characterized *in vivo*. Here, we have identified Ptpn9a, an ortholog of human PTPN9, as a crucial regulator of erythroid cell development in zebrafish embryos. *ptpn9a*, but not *ptpn9b*, was expressed in the posterior lateral plate mesoderm and intermediate cell mass – two primitive hematopoietic sites during zebrafish embryogenesis. Morpholino-mediated knockdown of *ptpn9a* caused erythrocytes to be depleted by inhibiting erythroid cell maturation without affecting erythroid proliferation and apoptosis. Consistently, both dominant-negative PTPN9 (with mutation C515S) and siRNA against *PTPN9* inhibited erythroid differentiation in human K562 cells. Mechanistically, depletion of *ptpn9* in zebrafish embryos *in vivo* or in K562 cells *in vitro* increased phosphorylated STAT3, and the hyper-phosphorylated STAT3 entrapped and prevented the transcription factors GATA1 and ZBP-89 (also known as ZNF148) from regulating erythroid gene expression. These findings imply that PTPN9 plays an important role in erythropoiesis by disrupting an inhibitory complex of phosphorylated STAT3, GATA1 and ZBP-89, providing new cellular and molecular insights into the role of *ptpn9a* in developmental hematopoiesis.

KEY WORDS: Erythroid cell development, PTPN9, STAT3, K562 cell

INTRODUCTION

Vertebrate hematopoiesis is a sequential process that occurs in primitive and definitive waves in anatomically distinct sites (Orkin and Zon, 2008). In mammals, primitive hematopoiesis occurs in the yolk-sac blood island, and definitive hematopoiesis originates in a distinct region known as the aorta-gonad-mesonephros (Cumano et al., 1996; Müller et al., 1994). In zebrafish, the primitive wave occurs in two intraembryonic regions, known as the anterior lateral plate mesoderm (ALPM) and the posterior lateral plate mesoderm (PLPM) that subsequently form the intermediate cell mass (ICM), whereas definitive hematopoiesis begins in the ventral wall of the dorsal

aorta (de Jong and Zon, 2005). The first wave produces primitive erythrocytes and macrophages, and the second wave generates hematopoietic stem cells (HSCs), which are self-renewing and pluripotent. HSCs migrate to the fetal liver and then to the bone marrow in mammals, but migrate to the caudal hematopoietic tissue and finally colonize at the kidney in zebrafish.

Primitive hematopoiesis is regulated by several transcription factors, including the stem cell leukemia gene (*SCL/TAL1*), the lim-only 2 gene (*LMO2*), *PU.1* (also known as *SP1*), *ZBP-89* (also known as *ZNF148*) and *GATA1*. By contrast, definitive hematopoiesis is initiated by the transcription factors RUNX1 and c-MYB (Paik and Zon, 2010). The importance of these factors has been demonstrated in cell-based *ex vivo* assays, as well as in knockout mouse models. SCL, a transcription factor with a basic helix-loop-helix motif, is a central regulator of hematopoietic differentiation. LMO2, a LIM domain transcription factor, acts in the same manner as SCL also in embryonic hematopoiesis (Gering et al., 2003; Shivdasani et al., 1995; Warren et al., 1994). The zinc finger protein ZBP-89 regulates hematopoietic progenitor cell differentiation (Li et al., 2006; Woo et al., 2008). Another zinc finger protein, GATA1, is specifically required for the maturation of proerythroblasts (Pevny et al., 1991). PU.1, a transcription factor that contains an ETS domain, plays an indispensable role in myeloid cell development (Scott et al., 1994). RUNX1, a runt domain transcription factor, is essential for the generation of HSCs in the ventral wall of the dorsal aorta (Chen et al., 2009; Kalev-Zylinska et al., 2002; Okuda et al., 1996). The myb-family member c-MYB maintains the population of HSCs in definitive hematopoiesis (Mucenski et al., 1991). These transcription factors form a sophisticated network in order to control the processes of primitive and definitive hematopoiesis.

Protein tyrosine kinases and protein tyrosine phosphatases (PTPs) play important roles in cell proliferation, differentiation, and migration through delicate regulation of signaling pathways. Human PTPN9 is a cytoplasmic phosphatase that is hyper-activated in erythroid progenitors in the bone marrow disorder polycythemia vera (Xu et al., 2003). Previous studies have shown that PTPN9 dephosphorylates NSF, FOXO1, ERBB2, EGFR and VEGFR2 for different functions, such as promoting homotypic vesicle fusion (Huynh et al., 2004), mediating insulin signaling in hepatocytes (Cho et al., 2006), suppressing breast cancer cell growth (Yuan et al., 2010) and regulating endothelial cell function (Hao et al., 2012). Recently, we have shown that PTPN9 directly interacts with STAT3 and mediates its dephosphorylation in breast cancer cells (Su et al., 2012). Overexpression of *PTPN9* decreases tyrosine phosphorylation of STAT3, whereas depletion of *PTPN9* increases its phosphorylation. Here, we show that PTPN9 has undergone duplication into *ptpn9a* and *ptpn9b* in

¹Beijing Key Laboratory of Cardiometabolic Molecular Medicine and State Key Laboratory of Natural and Biomimetic Drugs, Institute of Molecular Medicine, Peking University, Beijing, 100871 China. ²State Key Laboratory of Biomembrane and Membrane Biotechnology, School of Medicine, School of Life Sciences, Tsinghua University, Beijing, 100084 China. ³Institute of Medicinal Plant Development, Chinese Academy of Medical Sciences, Beijing, 100094 China. ⁴Beijing Shenogen Biomedical Company Ltd, Beijing, 100085 China.

*Authors for correspondence (kun.meng@shenogen.com; jingwei_xiong@pku.edu.cn)

zebrafish, and that *ptpn9a*, but not *ptpn9b*, regulates erythroid cell development by disrupting an inhibitory protein complex of phosphorylated STAT3, GATA1 and ZBP-89 in zebrafish embryos and human K562 cells.

RESULTS

ptpn9a is expressed in the primitive hematopoietic sites during zebrafish embryogenesis

To search for essential genes encoding PTPs downstream of zebrafish *cloche*, a classical mutant with hematopoietic and endothelial cell ablation (Stainier et al., 1995; Xiong et al., 2008), we performed an RNA *in situ* screen and then compared the expression of candidate genes between wild-type and *cloche* mutant embryos. From this screen, *ptpn9a* was downregulated in *cloche* mutants, which was further verified by semi-quantitative PCR analysis (data not shown). In the zebrafish genome, we found two homologs, *ptpn9a* and *ptpn9b*, of the human gene *PTPN9*. Zebrafish *ptpn9a* contains 13 exons and encodes 572 amino acids, which have 67% identity to human and mouse PTPN9. *ptpn9b* also contains 13 exons but encodes 716 amino acids, and the protein possesses a long stretch of linker sequences between the SEC14 and PTP catalytic (PTPc) domains – it displays 41% similarity to human and mouse PTPN9 (supplementary material Fig. S1A,B). Furthermore, synteny analysis revealed that zebrafish *snupn*, *ptpn9a* and *sin3aa* on chromosome 25, but not the zebrafish *ptpn9b* locus on chromosome 1, are conserved with their homologs on human chromosome 15 and mouse chromosome 9 (supplementary material Fig. S1C), suggesting that *ptpn9a*, but not *ptpn9b*, is the mammalian *PTPN9* ortholog in zebrafish.

We first assessed the expression patterns of *ptpn9a* and *ptpn9b* during zebrafish embryonic development by using RNA *in situ* hybridization. Both *ptpn9a* and *ptpn9b* were expressed maternally, and their expression was observed through the blastula and gastrulation stages (Fig. 1A,B; supplementary material Fig. S1D,E). After gastrulation, *ptpn9a* expression was evident in two primitive hematopoietic sites, the PLPM at 15 hours post fertilization (hpf) (Fig. 1C) and in the ICM (Fig. 1D), in addition to its expression in the developing brain at 18, 24 and 36 hpf (Fig. 1D–F). However, *ptpn9b* expression did not appear in the PLPM or the ICM (supplementary material Fig. S1F,G), and was predominantly expressed in the brain and somites

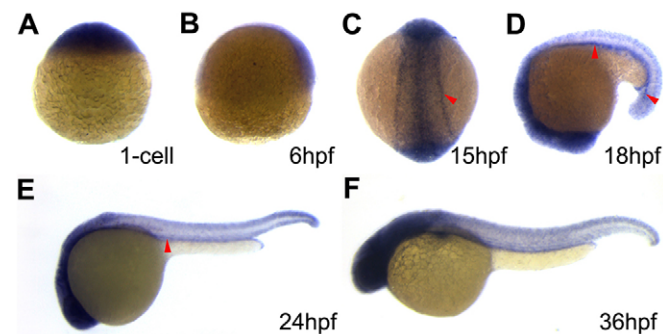


Fig. 1. *ptpn9a* is expressed in the primitive hematopoietic sites during zebrafish embryogenesis. RNA *in situ* hybridization with *ptpn9a* probe in one-cell (A), 6-hpf (B), 15-hpf (C), 18-hpf (D), 24-hpf (E) and 36-hpf (F) embryos. Note *ptpn9a* expression in the posterior lateral plate mesoderm (PLPM) (C; red arrowhead) and the intermediate cell mass (ICM) (D,E; red arrowheads) regions. Lateral views are shown with anterior to the left (D–F), and dorsal views are shown with anterior to the top (C).

through early embryogenesis (supplementary material Fig. S1G–I). We found that *ptpn9a* and *ptpn9b* were diffusely expressed in the trunk after 24 hpf, without enrichment in blood vessels or the ventral wall of the dorsal aorta (the definitive hematopoietic site) at 36 hpf (Fig. 1F; supplementary material Fig. S1I). Thus, these results suggest that *ptpn9a* is strongly associated with primitive hematopoiesis.

Knockdown of *ptpn9a* diminishes the number of primitive erythrocytes

To investigate the role of *ptpn9a* in primitive hematopoiesis, morpholino oligonucleotides against *ptpn9a* (*ptpn9a*-MOs) were injected into zebrafish embryos at the one- to two-cell stage. Most embryos tolerated the injection of 4 ng of morpholino oligonucleotide, but higher doses were toxic. *ptpn9a* morphants developed normally in the period up to 12 hpf but showed a short body length, ventrally curved tail and small head with moderate necrosis in the anterior region at 24 hpf (Fig. 2B). The number of circulating blood cells, as detected by *o*-Dianisidine staining, was greatly decreased in *ptpn9a*-MO-injected embryos (Fig. 2E) compared with that of wild-type embryos (Fig. 2D) at 48 hpf. Both the abnormal appearance and lack of erythrocytes were partially rescued in *ptpn9a* morphant embryos upon co-injection of human *PTPN9* mRNA (80 pg/embryo) (Fig. 2C,F), or zebrafish *ptpn9a* mRNA (100 pg/embryo) (supplementary material Fig. S1L–N). Neither *ptpn9b* nor SEC14-deleted *ptpn9a* mRNA was able to rescue the *ptpn9a* morphant phenotype (supplementary material Fig. S1O–T), supporting the notion of there being a specific role of *ptpn9a* in erythroid cell development. Using the transgene Tg[*gata1*:DsRed] (Traver et al., 2003) to label differentiated erythrocytes, we found that the DsRed-positive population was substantially reduced in *ptpn9a* morphants at 48 hpf (supplementary material Fig. S2S–T'). However, we did not see defects in primitive hematopoiesis after morpholino-oligonucleotide-mediated knockdown of *ptpn9b* in embryos (supplementary material Fig. S1J,K). Taken together, our data suggest that *ptpn9a*, but not *ptpn9b*, is essential for primitive hematopoiesis. To gain molecular insights into the hematopoietic hypoplasia in *ptpn9a* morphants, we investigated several known essential hematopoietic transcription factors. The transcription factors *scl/tal1*, *lmo2* and *flil1* are required for the generation of hematopoietic progenitors within the ALPM and PLPM (Gering et al., 2003; Liu et al., 2008). The expression of these three genes appeared to be unaffected in *ptpn9a*-knockdown embryos at 14 hpf (supplementary material Fig. S2A,C,E), suggesting that *ptpn9a* is not required for the generation of hematopoietic progenitors. However, the expression of the erythroid marker *gata1* was reduced in the PLPM at 15 hpf and in the ICM at 22 hpf in *ptpn9a*-MO-injected embryos (Fig. 2H,K), compared with that of wild-type embryos (Fig. 2G,J). Quantitative real-time PCR analysis further confirmed the diminished expression of the erythroid gene *gata1* (supplementary material Fig. S2W). Co-injection of human *PTPN9* mRNA fully rescued *gata1* expression in *ptpn9a* morphants (Fig. 2I,L). These observations confirm the hypothesis that *ptpn9a* is not required for the generation of hematopoietic progenitors but is crucial for their differentiation into erythrocytes.

We then addressed whether definitive hematopoiesis is affected in *ptpn9a* morphants. Depletion of either *runx1* or *cmyb* causes the complete absence of HSCs. We found that the populations of Runx1-positive and Cmyb-positive cells in the ventral wall of the dorsal aorta were unaltered in

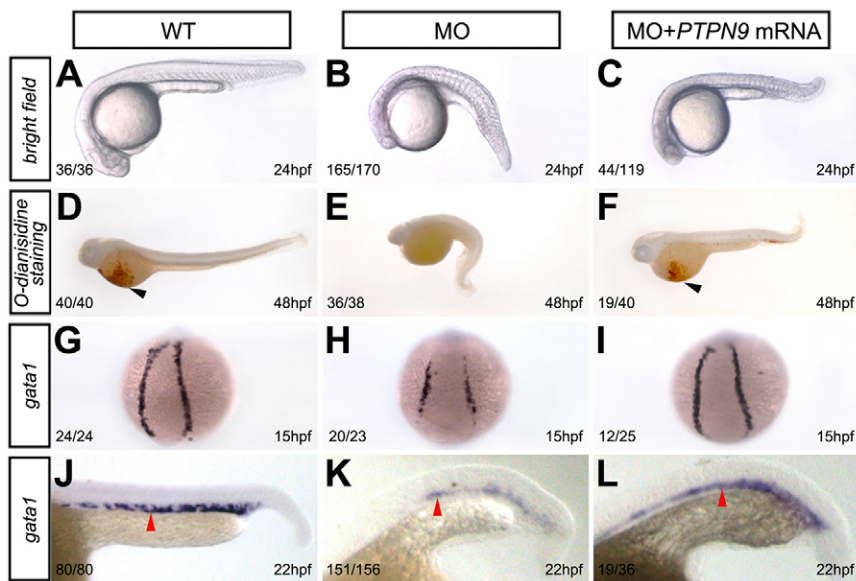


Fig. 2. Knockdown of *ptpn9a* depletes embryos of primitive erythrocytes. (A–C) Brightfield images of control (A), a *ptpn9a* morphant (MO) (B) and a *ptpn9a* morphant that had been co-injected with human *PTPN9* mRNA (C) at 24 hpf. (D–F) *o*-Dianisidine staining showed depletion of erythroid cells in *ptpn9a*-morphant embryos (E), compared with controls (D). Human *PTPN9* mRNA partially rescued primitive erythropoiesis in *ptpn9a*-morphant embryos (F). In D and F, black arrowheads indicate erythrocytes. (G–L) RNA *in situ* hybridization was performed with *gata1* probes in controls at 15 hpf (G) and 22 hpf (J), *ptpn9a* morphants at 15 hpf (H) and 22 hpf (K), and *ptpn9a* morphants that had been co-injected with human *PTPN9* mRNA at 15 hpf (I) and 22 hpf (L). Note reduced *gata1* expression in the PLPM (H) and ICM (K), which were partially rescued by co-injection of human *PTPN9* mRNA (I,L). Red arrowheads indicate the ICM (J–L). Lateral views are shown with anterior to the left (A–C, D–F, J–L); dorsal views are shown with anterior to the top (G–I). The number of phenotypic embryos/total embryos is shown in the bottom left-hand corner.

ptpn9a-MO-injected embryos at 36 hpf (supplementary material Fig. S2I–L). Consistently, HSCs were detected at normal levels in *ptpn9a* morphants using the Tg(*cd41*:GFP) and Tg(*cmyb*:GFP) transgenic embryos (Lin et al., 2005; North et al., 2007) (supplementary material Fig. S2U–V'; data not shown). Taken together, our results indicate that *ptpn9a* is not required for the specification of HSCs during embryogenesis.

Previous studies have shown that loss of *gata1* expression results in the ectopic expression of *pu.1*, resulting in the conversion of primitive erythropoiesis into myelopoiesis (Galloway et al., 2005; Rhodes et al., 2005). We found comparable levels of *pu.1* in the ALPM region of *ptpn9a*-MO-injected and wild-type embryos at 15 hpf (supplementary material Fig. S2G,H), as well as later in the ICM region at 22 hpf (data not shown). The expression of the myeloid genes *l-plastin*, myeloperoxidase (*mpo*) and lysozyme C (*lyz*) was mildly reduced in *ptpn9a* morphants (supplementary material Fig. S2N,P,R), compared with their expression in wild-type embryos (supplementary material Fig. S2M,O,Q). The mild reduction in the expression of myeloid genes in *ptpn9a* morphants was further verified using Tg(*mpo*:GFP) and Tg(*lyz*:dsRed) transgenic zebrafish, which have been widely used to label myeloid cells (Hall et al., 2007; Renshaw et al., 2006) (data not shown). Our observations suggest that the commitment to myeloid lineages develops normally, but that myeloid cell maturation is mildly affected, in *ptpn9a* morphants.

***ptpn9a* knockdown has no effect on erythroid cell proliferation and apoptosis in primitive hematopoiesis**

To investigate the cellular mechanisms underlying *ptpn9a*-morphant phenotypes, we examined hematopoietic cell proliferation and apoptosis in *ptpn9a*-knockdown embryos. The Tg(*ef1 α* :mAG-zGem) transgene has been shown to label S, G2 and M cells with green fluorescence (Sugiyama et al., 2009). We found comparable numbers of cells that were positive for green fluorescence in the ICM region in *ptpn9a*-MO-injected and wild-type Tg(*ef1 α* :mAG-zGem) transgenic embryos at 24 hpf (Fig. 3A,B). Furthermore, the number of apoptotic cells in the ICM region, revealed by using a terminal transferase UTP nick-end labeling (TUNEL) assay, was also comparable in *ptpn9a*

morphants and controls at 24 hpf (Fig. 3C,D). As expected, *p53* (also known as *tp53*) was not upregulated in the ICM region of *ptpn9a*-knockdown embryos (Fig. 3F). Co-injection of both *ptpn9a*-MOs and *p53*-MOs did not reverse the morphology, or the *gata1* expression, in *ptpn9a* morphants (data not shown). To determine whether human *PTPN9* also plays a similar role in mammalian developmental hematopoiesis, we used hemin in a differentiation system in order to induce K562 hematopoietic progenitors into mature erythrocytes. Consistently, inhibition of *PTPN9* – by using either catalytically inactive dominant-negative

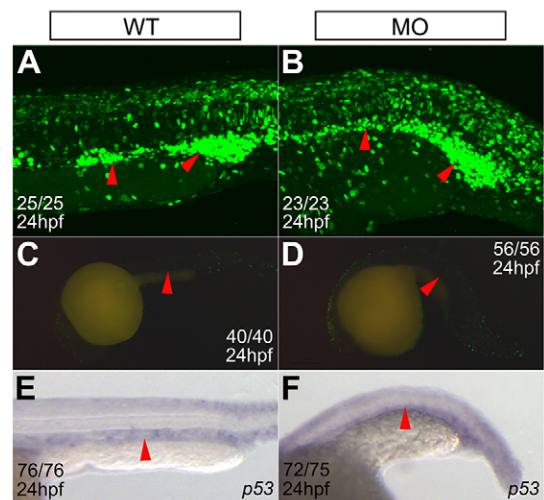


Fig. 3. *ptpn9a* knockdown causes no defect in hematopoietic cell proliferation and apoptosis. (A,B) *ptpn9a*-MOs were injected into Tg(*ef1 α* :mAG-zGem) transgenic embryos, in which green-fluorescence-positive cells are in phases S, G2 or M of the cell cycle. Note that there is little difference in the numbers of green-fluorescence-positive cells in the ICM between *ptpn9a*-morphant (B) and wild-type (A) embryos at 24 hpf. (C,D) The TUNEL assay showed comparable numbers of apoptotic cells in the ICM in *ptpn9a* morphants (D) and controls (C) at 24 hpf. (E,F) RNA *in situ* hybridization revealed that expression of the *p53* gene was not induced in the ICM of *ptpn9a*-morphant embryos (F), compared with wild-type controls (E). Red arrowheads indicate the ICM. The number of phenotypic embryos/total embryos is indicated.

PTPN9 (N9CS), which carried a mutation of cysteine residue 515 to serine, or PTPN9 siRNA (shN9) – had no effect on human K562 cell apoptosis (supplementary material Fig. S3A–F) and hemin-induced K562 cell proliferation (supplementary material Fig. S3G). These observations suggest that *ptpn9a* is not required for erythroid cell proliferation and apoptosis.

PTPN9 is required for erythroid cell maturation

We then hypothesized that *ptpn9a* might play a role in erythroid cell maturation. We chose to investigate the expression pattern of two markers of the terminal differentiation of erythrocytes, *βe1-globin* and *βe2-globin* (also known as *hbbe1* and *hbbe2*, respectively), during primitive hematopoiesis. The expression of both genes gradually diminished from 26 to 48 hpf in *ptpn9a* morphants (Fig. 4A,C,E,G,I) compared with that in controls (Fig. 4B,D,F,H,J). Quantitative real-time PCR analysis further confirmed the diminished expression of erythroid genes, including *βe1-globin* and *βe2-globin* (supplementary material Fig. S2Y,Z). Co-injection of human *PTPN9* mRNA (80 pg per

embryo) or zebrafish *ptpn9a* mRNA (100 pg per embryo) rescued the expression of *βe1-globin* in *ptpn9a*-MO-injected embryos (Fig. 4K,L; supplementary material Fig. S1L–N). We conclude that in *ptpn9a*-knockdown embryos primitive hematopoiesis is initiated, whereas the differentiation of hematopoietic progenitors into erythroid cells is blocked, resulting in the accumulation of immature erythroid cells.

We then used the differentiation system in order to induce K562 hematopoietic progenitors into mature erythrocytes in the presence of hemin. Compared with vector controls, we found that inhibition of PTPN9 function by a dominant-negative form of PTPN9 (N9CS) significantly reduced the percentage of benzidine-positive erythrocytes (Fig. 4M). Consistently, knockdown of *PTPN9*, by stably silencing *PTPN9* in K562 cells with specific RNA interfering constructs (shN9), also led to a reduction of benzidine-positive erythrocytes (Fig. 4M). The short hairpin construct termed ShN9-3 was the most potent short hairpin among three RNAi constructs (supplementary material Fig. S4B). Furthermore, quantitative real-time PCR revealed that

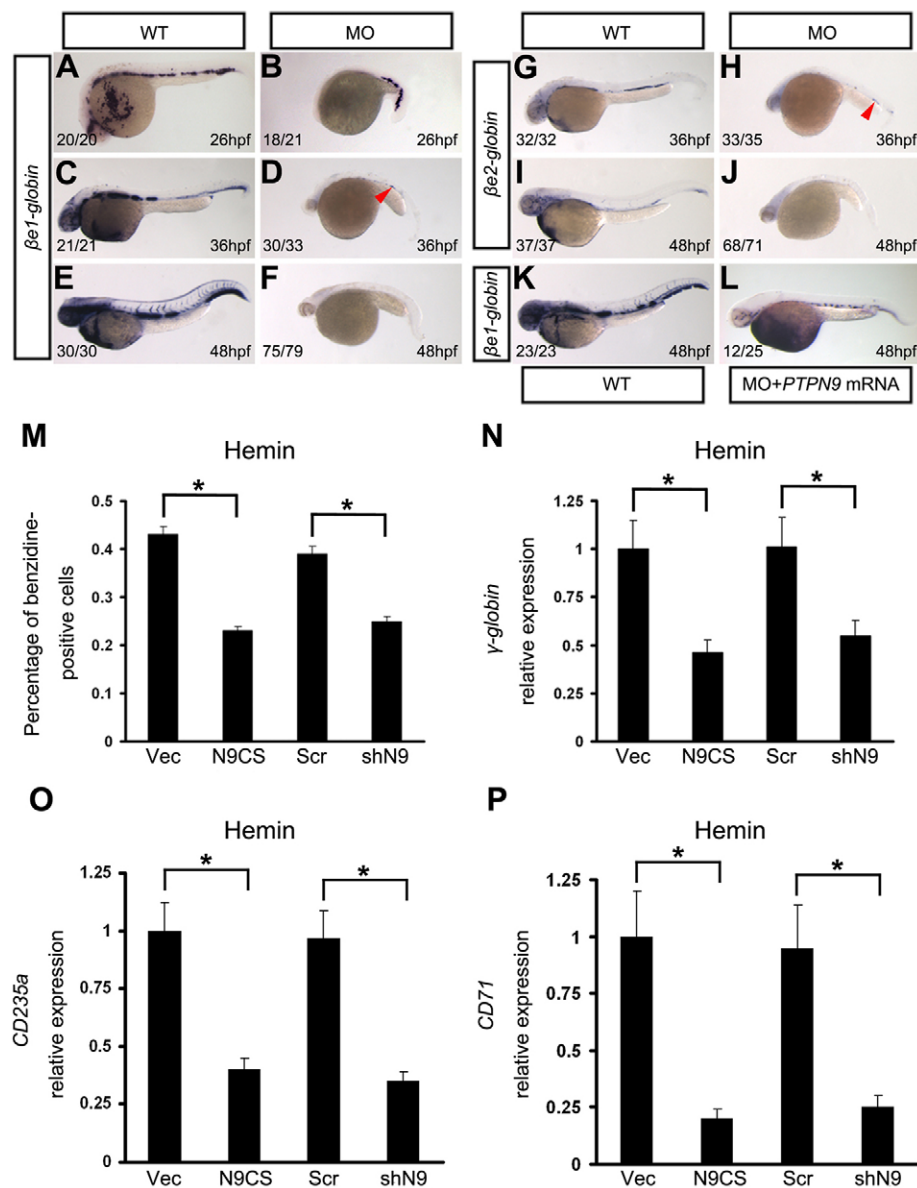


Fig. 4. Knockdown of *PTPN9* interferes with erythroid cell maturation. RNA *in situ* hybridization was performed with *βe1-globin* (A–F,K,L) or *βe2-globin* (G–J) in controls (A,C,E,G,I,K) or *ptpn9a* morphants (B,D,F,H,J,L). Note the reduced *βe1-globin* at 26 hpf (B) and substantially diminished *βe1-globin* at 36 hpf (D) and at 48 hpf (F) in *ptpn9a* morphants, compared with controls (A,C,E). *βe2-globin* was almost abolished at 36 hpf (H) and 48 hpf (J) in *ptpn9a* morphants, compared with controls (G,I). Overexpression of human *PTPN9* mRNA partially rescued *βe1-globin* in *ptpn9a* morphant embryos at 48 hpf (L), compared with controls (K). Lateral views are shown with anterior to the left (A–L). Red arrowheads indicate *βe1-globin*-positive or *βe2-globin*-positive erythrocytes at 36 hpf (D,H). The numbers in the bottom left-hand corners indicate the phenotypic embryos/total embryos. (M–P) Human K562 cells were infected with retroviruses containing either an empty vector (Vec) or a dominant-negative mutant *PTPN9* (N9CS), or were transfected with either a scrambled construct (Scr) or *PTPN9* RNAi construct (shN9). The infected or transfected K562 cells were induced with hemin for 48 h. (M) The percentages of benzidine-positive cells were reduced in both N9CS and shN9 groups. Error bars represent the standard deviation, and the means of data from three independent experiments are shown. (N–P) Quantitative real-time PCR analyzed the expression of *γ-globin*, *CD235a* and *CD71* in infected or transfected K562 cells after hemin induction for 48 h. Relative *γ-globin*, *CD235a* and *CD71* expression levels, normalized to *GAPDH*, were reduced in both N9CS and shN9 groups. Measurements are the means from three independent experiments \pm s.d., * $P < 0.05$.

hemin-induced expression of the erythroid genes encoding γ -globin (here, specifically, *HBG2*), *CD235a* (also known as *GYP A*) and *CD71* (also known as *TFRC*) was inhibited in K562 cells that expressed N9CS or shN9 (Fig. 4N–P). Taken together, these data suggest that PTPN9 is required for erythroid cell maturation.

Increased STAT3 phosphorylation by knockdown of *PTPN9* enhances formation of the STAT3–GATA1–ZBP-89 complex

Our previous work has shown that PTPN9 directly dephosphorylates STAT3 in breast cancer cells (Su et al., 2012). Because *STAT3* plays an important role in mammalian hematopoiesis, we hypothesized that Ptpn9a might also dephosphorylate Stat3 during zebrafish hematopoiesis. We found that *ptpn9a* knockdown increased, whereas overexpression of *ptpn9a* decreased, Stat3 phosphorylation in zebrafish embryos at 18 hpf (Fig. 5A). By contrast, *ptpn9b* knockdown had no effect on the phosphorylation of Stat3 in zebrafish (supplementary material Fig. S4A). In human K562 cells, STAT3 phosphorylation was also increased after overexpression of the dominant-negative PTPN9 mutant N9CS (Fig. 5B; supplementary material Fig. S4C) or transfection with *PTPN9* RNAi constructs (shN9) (supplementary material Fig. S4B). These data suggest a possible direct dephosphorylation of STAT3 by PTPN9 in zebrafish embryos and human K562 cells.

To demonstrate a physical interaction between PTPN9 and STAT3, FLAG-tagged wild-type STAT3 or FLAG-tagged dominant-negative mutant STAT3 (with the mutation Y705F) (Rong et al., 2006) was co-transfected with Myc-tagged PTPN9 (Myc–PTPN9) into 293T cells. In the presence of IL-6 and soluble IL-6 receptor after transfection, the protein complex was isolated by immunoprecipitation by using an antibody against FLAG. These experiments revealed that both endogenous PTPN9 (Fig. 5C) and overexpressed Myc–PTPN9 physically associated with STAT3 and preferentially bound to wild-type STAT3 (supplementary material Fig. S4D). Previous studies have shown that formation of the STAT3–GATA1 complex leads to the inhibition of the expression of γ -globin (Ezoe et al., 2005; Foley et al., 2002; Kirito et al., 1998; Yao et al., 2009). Furthermore, the Krüppel-type zinc finger transcription factor ZBP-89 has been previously reported to interact with GATA1 and regulate expression of the globin genes and erythroid differentiation during hematopoiesis in zebrafish (Li et al., 2006; Ohneda et al., 2009; Woo et al., 2011; Woo et al., 2008). Based on these studies, we hypothesized that STAT3, GATA1 and ZBP-89 might form a multiprotein complex to regulate erythroid differentiation. Indeed, we found that endogenous STAT3 interacted with GATA1 and ZBP-89 (Fig. 5D; supplementary material Fig. S4H). Myc–GATA1 preferentially interacted with FLAG-tagged wild-type, but not dominant-negative, STAT3, indicating that the interaction requires activation of STAT3 phosphorylation. We also showed that ZBP-89 interacted with active STAT3 (supplementary material Fig. S4E,F) and that there is a physical interaction between GATA1 and ZBP-89 in murine erythroleukemia (MEL) cells, which is consistent with a previous report (Woo et al., 2008) (supplementary material Fig. S4G).

Owing to the inhibitory effect of phosphorylated STAT3 on erythroid cell maturation (Foley et al., 2002; Yao et al., 2009), we assumed that knockdown of *PTPN9* might increase STAT3 phosphorylation and formation of the STAT3–GATA1–ZBP-89 complex, which prevents binding of GATA1 and ZBP-89 to

the promoters of their target genes. We found that increased STAT3 phosphorylation, by overexpression of dominant-negative N9CS, led to the recruitment of more GATA1 and ZBP-89 into the complex (Fig. 5E). By contrast, decreasing phosphorylated STAT3 by overexpression of wild-type PTPN9 prevented formation of the phosphorylated STAT3, GATA1 and ZBP-89 complex (Fig. 5E). Consistent with these results, we found that increasing phosphorylated STAT3, by using shN9 knockdown, caused the formation of more phosphorylated STAT3, GATA1 and ZBP-89 complexes than in controls (Fig. 5F). As predicted, we further showed that inhibition of PTPN9 by either N9CS or shN9 decreased the binding of GATA1 to its target genes γ -globin and *CD235a* by using chromatin immunoprecipitation assays, which was fully rescued by co-transfection of dominant-negative STAT3 (Fig. 5G,H). In addition, PTPN9 knockdown by *ptpn9a*-MO in zebrafish, or abrogation of its function, by using N9CS and shN9, in human K562 cells decreased the expression of GATA1 but not STAT3 and ZBP-89 (Fig. 2G,H; Fig. 5A; supplementary material Fig. S2W–X and Fig. S4I,J,M,N). GATA1 knockdown in K562 cells reduced the complex formation but had no effect on the expression of phosphorylated STAT3, total STAT3 and ZBP-89 (supplementary material Fig. S4K), and ZBP-89 knockdown in K562 cells decreased the complex formation but slightly reduced GATA1 levels and had no effect on phosphorylated STAT3 and total STAT3 (supplementary material Fig. S4L). These data strongly support the notion that STAT3 phosphorylation, which is negatively regulated by PTPN9, is crucial for the formation of an inhibitory protein complex comprising phosphorylated STAT3, GATA1 and ZBP-89.

Dephosphorylation of STAT3 by PTPN9 contributes to erythroid cell maturation

To further test our hypothesis on the inhibitory protein complex of phosphorylated STAT3, GATA1 and ZBP-89, we investigated erythroid cell maturation by manipulating the levels of phosphorylated STAT3, GATA1 or ZBP-89 in zebrafish embryos and human K562 cells. Remarkably, overexpression of *gatal* (50 pg per embryo), *zbp-89* (100 pg per embryo) or human dominant-negative *STAT3* (50 pg per embryo) partially rescued β 1-globin expression in *ptpn9a* morphants (Fig. 6C,I,L). Additionally, overexpression of *gatal* rescued erythroids, as identified by *o*-Dianisidine staining, in *ptpn9a* morphants (Fig. 6F). In K562 cells expressing N9CS or shN9, upon treatment with hemin for 48 h, we consistently found that overexpression of dominant-negative *STAT3* partially rescued the number of benzidine-positive erythroid cells and the expression of erythroid genes γ -globin, *CD235a* and *CD71* (Fig. 6M–P), whereas overexpression of dominant-negative *STAT3* or constitutively active *STAT3* alone had no effect on K562 cell proliferation (supplementary material Fig. S3I). Consistently, overexpression of constitutively active *STAT3* decreased the benzidine-positive erythroids upon treatment with hemin for 48 h (supplementary material Fig. S3J). However, we found that decreasing STAT3 phosphorylation by overexpression of either wild-type PTPN9 or dominant-negative *STAT3* alone had no effect on the formation of benzidine-positive erythroids after the induction of maturation upon treatment with hemin for 48 h (supplementary material Fig. S3H,J). Taken together, we conclude that PTPN9 plays a crucial role in erythroid cell maturation by dephosphorylating STAT3.

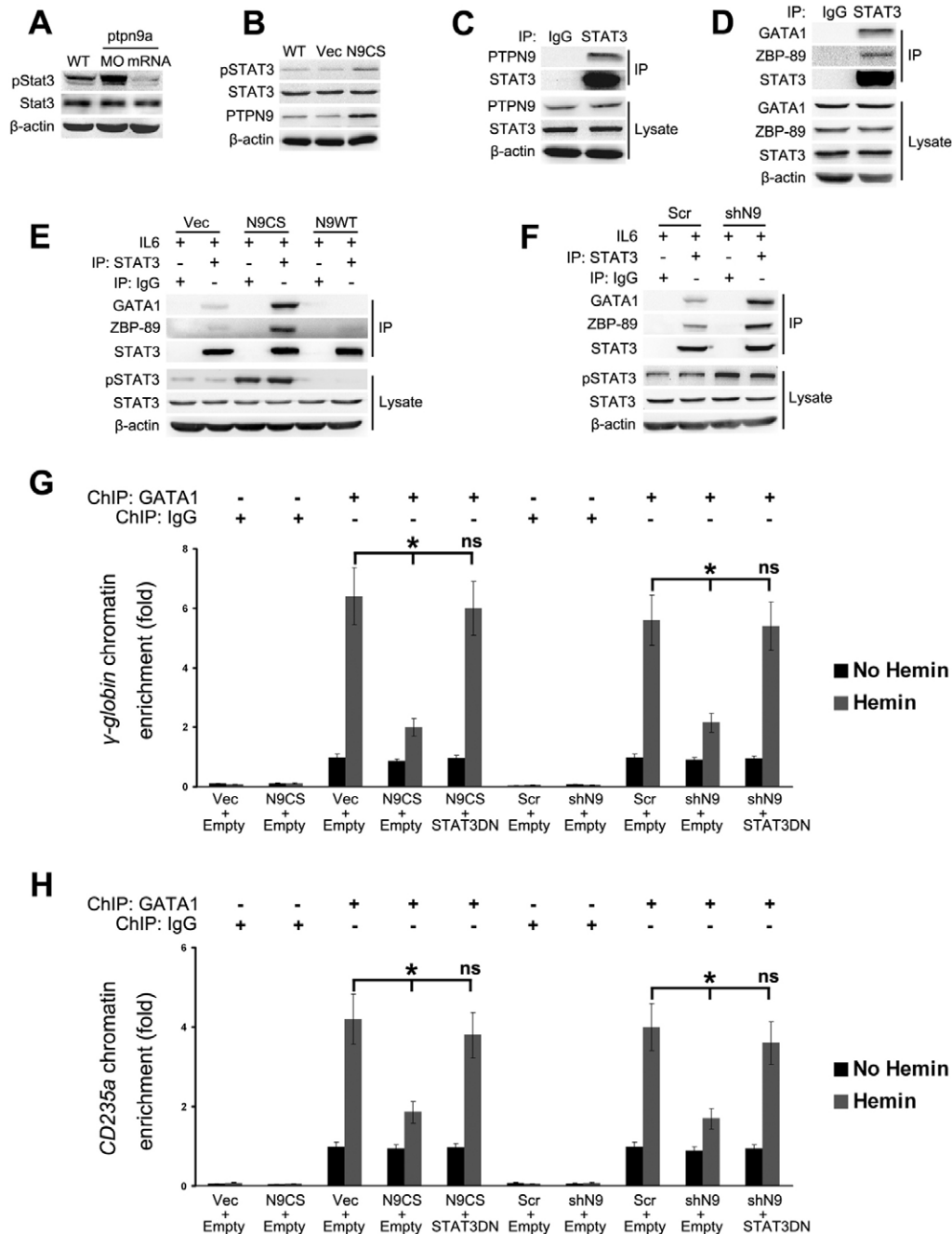


Fig. 5. Increasing phosphorylated STAT3 by *PTPN9* knockdown stimulates the formation of an inhibitory complex comprising phosphorylated STAT3, GATA1 and ZBP-89 and reduces the GATA1 binding activity. (A) The phosphorylation (pStat3) status of endogenous Stat3 protein was elevated in *ptpn9a*-morphant (MO) embryos but reduced in *ptpn9a*-mRNA-injected embryos (mRNA), compared with wild-type (WT) embryos at 18 hpf, as shown by western blotting. The total amounts of Stat3 were relatively unchanged. (B) Endogenous phosphorylated STAT3, as shown by western blotting, was increased in human K562 cells that had been infected with the dominant-negative mutant PTPN9C515S (N9CS), compared with uninfected cells (WT) or cells infected with an empty vector (Vec). (C) The STAT3 protein complex, immunoprecipitated (IP) by using an antibody against STAT3, contained PTPN9, suggesting that endogenous PTPN9 physically interacts with STAT3 in K562 cells. IgG, control IP. (D) The endogenous STAT3 protein complex, immunoprecipitated by using an antibody against STAT3, contained GATA1 and ZBP-89, suggesting that endogenous STAT3 physically interacts with GATA1 and ZBP-89 in K562 cells. (E) Overexpression of the dominant-negative mutant PTPN9 (N9CS) in K562 cells increased phosphorylated STAT3 and promoted the formation of the phosphorylated-STAT3–GATA1–ZBP-89 complex, whereas overexpression of wild-type PTPN9 (N9WT) decreased phosphorylated STAT3 and the protein complex, compared with the vector control (Vec) group. (F) *PTPN9* knockdown (shN9) also increased phosphorylated STAT3 and promoted the formation of the phosphorylated-STAT3–GATA1–ZBP-89 complex, compared with a scrambled construct (Scr) in K562 cells. K562 cells were induced by using IL-6 for 6 h before cell lysates were prepared for immunoprecipitation with an antibody against STAT3. (G,H) Overexpression of either dominant-negative mutant PTPN9 (N9CS) or *PTPN9* knockdown (shN9) in K562 cells reduced the binding of GATA1 to its target genes γ -globin and *CD235a*, compared with vector (Vec) or scrambled (Scr) controls. Overexpression of dominant-negative STAT3 (STAT3DN) rescued the binding of GATA1 to its target genes in K562 cells that had been infected with mutant PTPN9 (N9CS) or transfected with *PTPN9* shRNA (shN9). ChIP assays were performed using an antibody against GATA1 or IgG control. Quantitative PCR was used to evaluate the promoter occupancy of γ -globin and *CD235a* by GATA1 protein with or without treatment with hemin. The data are the means from three independent experiments \pm s.d.; * $P < 0.05$; ns, not significant.

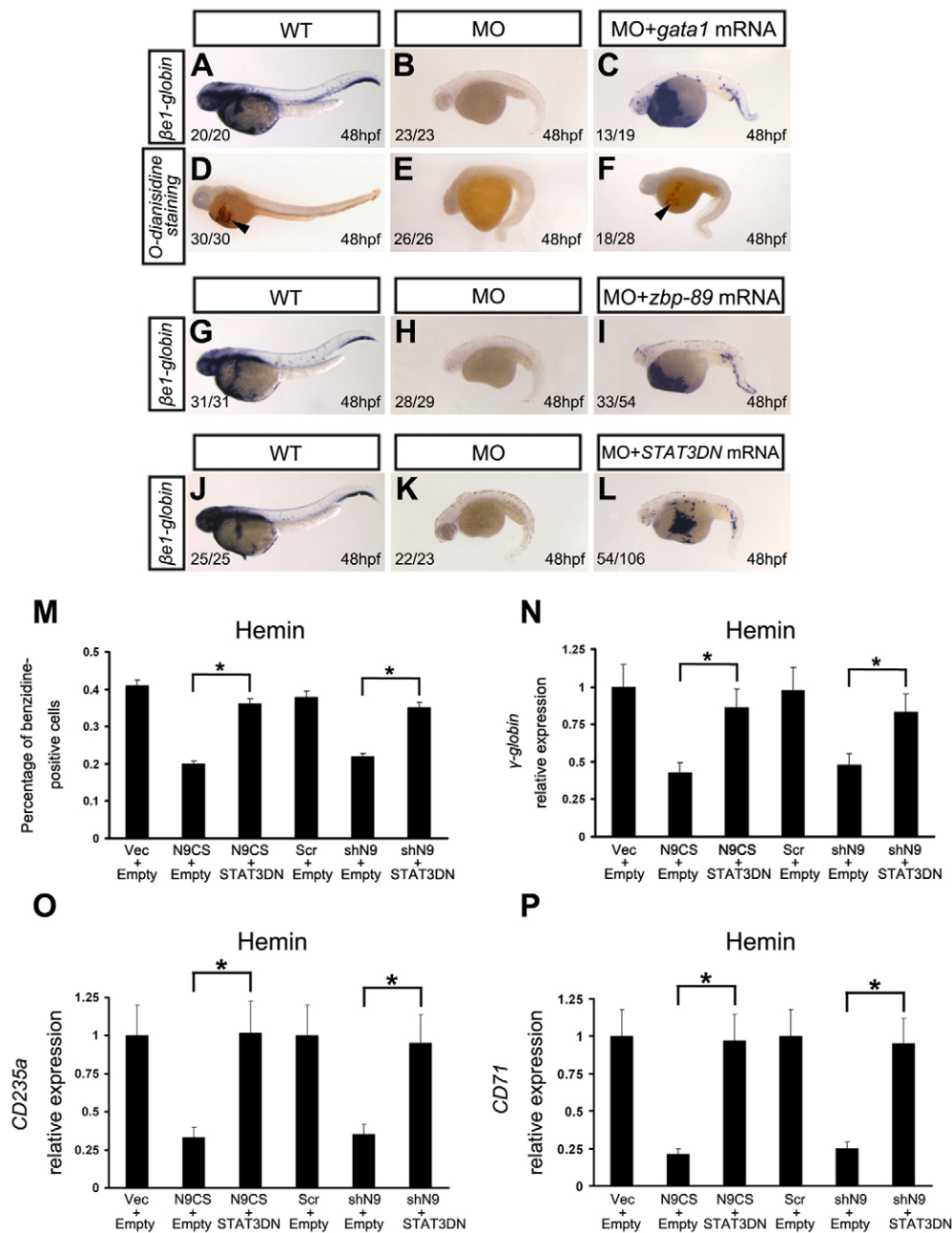


Fig. 6. Overexpressing *gata1*, *zbp-89* or dominant-negative *STAT3* rescues erythroid development in *ptpn9a*-morphant embryos and *PTPN9*-knockdown K562 cells.

(A–C,G–L) $\beta e1$ -globin was partially rescued in *ptpn9a* morphants (MO) that had been co-injected with *gata1* mRNA (C), *zbp-89* mRNA (I) or dominant-negative *STAT3* (*STAT3DN*) mRNA (L), compared with wild-type (WT) controls (A,G,J) at 48 hpf. In addition, overexpression of *gata1* mRNA rescued primitive erythrocytes in *ptpn9a* morphants (F), compared with wild-type controls (D), as revealed by O-Dianisidine staining. The numbers in the bottom left corner represent phenotypic embryos/total embryos.

(M–P) Overexpression of *STAT3DN* rescued benzidine-positive erythrocytes (M) and γ -globin (N), *CD235a* (O) and *CD71* (P) expression in K562 cells that had been infected with either mutant *PTPN9* (N9CS) or transfected with *PTPN9* shRNA (shN9) after induction with hemin for 48 h, compared with vector (Vec) or scrambled (Scr) controls. The data represent the means of three independent experiments \pm s.d., * $P < 0.05$.

DISCUSSION

In this study, we have demonstrated that *PTPN9* functions in erythropoiesis in both zebrafish embryos and human K562 cells by regulating the differentiation of hematopoietic progenitors into erythrocytes and that *PTPN9* acts through dephosphorylating *STAT3*, preventing the formation of an inhibitory protein complex comprising phosphorylated *STAT3*, *GATA1* and *ZBP-89*. Erythrocyte hypoplasia was not caused by defects in either erythroid cell proliferation or apoptosis but was mainly due to a deficiency in erythroid cell maturation in *ptpn9a*-knockdown zebrafish embryos and K562 cells that lacked functional *PTPN9*. We note that *PTPN9* plays an essential role in the formation of erythroid colonies derived from human embryonic stem cells or human endothelial colony-forming cells (Huang et al., 2011; Xu et al., 2003). Because human *PTPN9* was able to partially rescue *ptpn9a*-morphant phenotypes in zebrafish, we suggest that the

two genes have conserved functions in erythroid maturation. We also found that the number of myeloid cells was decreased in *ptpn9a* morphants but could not be rescued by overexpression of a moderate dose of human dominant-negative *STAT3* mRNA (data not shown), suggesting that other downstream target proteins of *PTPN9* are involved in the regulation of myeloid cell maturation.

Mechanistically, we demonstrated that knockdown of *PTPN9* increased *STAT3* phosphorylation and then impaired erythroid cell development through the inhibition of erythroid gene expression by *GATA1* and *ZBP-89*. Previous studies have elucidated that phosphorylated *STAT3* inhibits *GATA1* through a direct protein–protein interaction (Ezoe et al., 2005; Yao et al., 2009). The ability of phosphorylated *STAT3* to suppress *GATA1* transactivation has been attributed to the alteration of *GATA1* binding stability. At present, it remains to be determined whether

the same mechanism is involved in the relationship between phosphorylated STAT3 and ZBP-89. Signal transducers and activators of transcription (STAT) proteins are transcription factors that are activated by phosphorylation on tyrosine residues after cytokine stimulation. During erythropoiesis, Janus kinase 2 (JAK2) transduces erythropoietin (EPO) signals to enhance erythroid cell proliferation and differentiation by phosphorylating STAT5 and STAT3. In zebrafish, knockdown of *epo* or *jak2a* decreases primitive erythropoiesis (Ma et al., 2007; Paffett-Lugassy et al., 2007). Our preliminary experiments revealed that STAT5 and STAT3 were tyrosine-phosphorylated by EPO stimulation in K562 cells (data not shown). After EPO stimulation, we noted that STAT3 phosphorylation was increased in K562 cells that expressed mutant PTPN9 (N9CS), a response similar to that seen in response to IL6 stimulation, shown in supplementary material Fig. S4C. However, STAT5 phosphorylation was unchanged in this condition, which is consistent with our previous observation that PTPN9 interacts very weakly with STAT5 (Su et al., 2012). Another study showed that PTPN9 preferentially associates with JAK1 but not TYK2 and JAK2 (Hao et al., 2012). Considering these findings together, we favor the notion that PTPN9 predominantly dephosphorylates STAT3 in erythropoiesis, which is different from the targets of other phosphatases such as SHP-1, SHP-2 and CD45 (also known as PTPN6, PTPN11 and PTPRC, respectively) (Valentino and Pierre, 2006). SHP-1 has been shown to dephosphorylate JAK2 through an interaction with GRB2 (Minoo et al., 2004) and directly dephosphorylate STAT5 in a PLC- β 3-dependent manner (Xiao et al., 2009). Mice deficient for *Shp-1* display high proliferation of all hematopoietic lineages. Zebrafish *shp-1* (*ptpn6*) is only expressed in myeloid cells during hematopoiesis (Zakrzewska et al., 2010). SHP-2, a widely distributed phosphatase, is associated with EPO receptor, c-KIT and GP130 (also known as IL6ST) in hematopoietic cells (Tauchi et al., 1996; Tauchi et al., 1994). Deletion of the *Shp-2* gene is embryonic lethal in mice, and mutations of *SHP-2* cause human Noonan syndrome. In zebrafish, *shp-2* (*ptpn11*) is expressed ubiquitously during embryogenesis with the highest expression in the developing central nervous system and spinal cord (Jopling et al., 2007; Stewart et al., 2010). CD45, specifically expressed in hematopoietic cells, regulates T-cell and B-cell antigen receptor signaling. *CD45*-knockout mice show a loss of antigen responses in T and B lymphocytes. In zebrafish, *cd45* marks a subset of aortagonad-mesonephros HSCs and differentiated leukocytes (Bertrand et al., 2008). Therefore, the temporal and spatial expression of phosphatases and their targets determine the specificity and roles of phosphatases in hematopoietic development.

Normal levels of STAT3 phosphorylation are required for maintaining erythroid cell proliferation during embryonic development (Jenkins et al., 2002; Jenkins et al., 2005; Kiritto et al., 1998; Mantel et al., 2012; Welte et al., 2003). However, our work showed that hyper-phosphorylated STAT3 impaired erythroid cell maturation in zebrafish and human K562 cells. In *Gp130*^{Y757E/Y757F} mutant mice, GP130-dependent STAT3 hyperactivation results in increased numbers of hematopoietic progenitor cells (Jenkins et al., 2005). In *Gp130*^{ΔΔ} mice, which contain a C-terminal truncation mutation in GP130 that eliminates GP130-mediated STAT3 activation, hematopoietic progenitor cells – including committed erythroid progenitors – are also increased (Jenkins et al., 2002). Endothelial deletion of STAT3 in mice bred from homozygous *Stat3-loxP* mice and *Tie2-Cre* mice causes defects in hematopoietic stem cell

proliferation and differentiation, leading to erythroid dysplasia and increased myeloproliferation (Mantel et al., 2012; Welte et al., 2003). These studies indicate that STAT3 plays a crucial role in definitive hematopoiesis. Taken together with our data presented here and the work of others, we propose that STAT3 phosphorylation, under the control of different phosphokinases and phosphatases, plays different roles in primitive and definitive hematopoiesis and that, in zebrafish, Ptpn9 might interact with different substrates in order to regulate primitive and definitive hematopoiesis.

MATERIALS AND METHODS

Fish maintenance

Tg(*eflα*:mAG-zGem) transgenic reporter zebrafish for the S, G2 and M phases of the cell cycle were generated, as described previously (Sugiyama et al., 2009). Tg(*gatal*:DsRed) were kindly provided by Shuo Lin (University of California Los Angeles, Los Angeles, CA). Tg(*mpo*:GFP), Tg(*lyz*:dsRed), Tg(*cd41*:GFP) and Tg(*cmyb*:GFP) zebrafish were provided by Zilong Wen (Hong Kong University of Science and Technology, Hong Kong, China). Wild-type Tupfel long fin, AB and transgenic zebrafish were raised and handled in accordance with the guidelines of the Peking University Institutional Animal Care and Use Committee accredited by the Association for Assessment and Accreditation of Laboratory Animal Care.

Constructs

The zebrafish *ptpn9a* and *ptpn9b* genes were amplified and subcloned into vector pEASY Blunt and pXT7 for antisense probe and mRNA synthesis. SEC14-deleted *ptpn9a* cDNA was cloned into the pXT7 vector, which was used as a template for mRNA synthesis. Plasmid clones for the generation of probes of zebrafish *runx1*, *cmyb*, *βe1-globin*, *lmo2* and *mpo* were kindly provided by Feng Liu (Institute of Zoology, Beijing, China). Other plasmid clones for generating probes of zebrafish *gatal*, *scl*, *pu.1*, *l-plastin*, *βe2-globin*, *lyz*, *bmp4* and *notch1b* were stocks from our laboratory. Constructs for mRNA synthesis (zebrafish *gatal* and *zbp-89*) and protein expression (human *GATA1* and *ZBP-89*) were kindly provided by Xiangen Li (Harvard University, Cambridge, MA) (Li et al., 2006). shRNA against human *GATA1* (shGATA1) and human *ZBP-89* (shZBP-89) were designed as described previously (Woo et al., 2011). Human PTPN9, PTPN9C515S (a dominant-negative mutant of human PTPN9; N9CS), STAT3, STAT3Y705F (a dominant-negative STAT3), STAT3CA (constitutively active STAT3 with the double mutation A661C N663C) and shPTPN9 (shRNA against human PTPN9; shN9) constructs have been described previously (Su et al., 2012).

Morpholinos, mRNA synthesis and microinjection

The following morpholino antisense oligonucleotides were purchased from Gene Tools and suspended as 2 mM stocks in RNase-free water. The sequences of *ptpn9a*-MO, *ptpn9b*-MO and *p53*-MO are available in supplementary material Table S1. Capped mRNAs were synthesized from linearized pXT7 constructs using the mMessage mMachine kit (Ambion). In all the microinjection experiments, a volume of 2.3 nl was injected into one- to two-cell-stage embryos.

Whole-mount *in situ* hybridization, o-Dianisidine staining and TUNEL assay

Antisense probes were synthesized using the DIG RNA labeling kit (Roche) according to the manufacturer's instructions, as described previously (Xiong et al., 2008). o-Dianisidine staining has been reported previously (Danilova et al., 2011). TUNEL was performed using the *In Situ* Cell Death Detection Kit and TMR Red (Roche) according to the manufacturer's instructions.

Cell culture, infection, transfection, Hoechst 33342 and benzidine staining

K562 cells and MEL cells were cultured in 1640 medium. Hemin (50 μM, Sigma-Aldrich) was used to induce erythroid differentiation in K562 cells. Human recombinant IL-6 (100 ng/ml, R&D Systems) and human

recombinant EPO (50 U/ml, R&D Systems) were used to stimulate K562 cells. K562 cells were infected with the retroviruses pMSCV-vector, pMSCV-PTPN9WT or pMSCV-PTPN9C515S. K562 cells (1×10^7 cells) were electroporated at 280 V and 975 μ F with 20 μ g of non-linearized plasmid (STAT3Y705F, STAT3CA, shGATA1, shZBP-89 and shPTPN9 constructs) using Gene-Pulser II (Bio-Rad). Stable cell-lines were selected with 0.6 mg/ml G418 and 1 μ g/ml puromycin. HEK 293T cells were cultured in Dulbecco's modified Eagle's medium and transient transfection was performed using LipofectamineTM 2000 (Invitrogen) according to the manufacturer's instructions. Human recombinant IL-6 and IL-6 receptor (100 ng/ml, R&D Systems) were used to stimulate 293T cells. Benzidine staining has been reported previously (Cooper et al., 1974).

Semi-quantitative and real-time RT-PCR

Total RNA was isolated from embryos at different stages, or from harvested cells, using Trizol (Invitrogen). First-strand cDNA was synthesized from 2 μ g of total RNA by SuperScript II RT (Life Technologies) according to the manufacturer's protocol. Quantitative real-time PCR was performed using an iQ5 real-time PCR detection system (Bio-Rad) and a SYBR Premix Ex Taq kit (Takara). Primer sequences are listed in supplementary material Table S1.

Western blot, chromatin immunoprecipitation and immunoprecipitation

Zebrafish embryos were lysed in modified radio-immunoprecipitation assay (RIPA) lysis buffer that had been supplemented with protease and phosphatase inhibitors (50 mM Tris-HCl pH 7.4, 0.25% sodium deoxycholate, 1% NP-40, 150 mM NaCl, 1 mM EDTA, 1 mM PMSF). K562 cells, MEL cells and 293T cells were harvested and used for immunoprecipitation reactions, as described previously (Hu et al., 2006). Chromatin immunoprecipitation (ChIP) assays were performed by using PierceTM agarose ChIP kit according to the manufacturer's protocol. FLAG-M2-antibody-conjugated beads (Sigma-Aldrich) were used for immunoprecipitation. The following antibodies against the indicated proteins were also used in this study: zebrafish phosphorylated Stat3 (Tyr708) (Medical and Biological Laboratories), STAT3 (C-20, Santa Cruz Biotechnology), β -actin (Cell Signaling Technology), phosphorylated Stat3 (Tyr705, D3A7) (Cell Signaling Technology), Stat3 (124H6, Cell Signaling Technology), GATA1 (D52H6, Cell Signaling Technology), ZBP-89 (H-7, Santa Cruz Biotechnology), ZBP-89 (S-15, Santa Cruz Biotechnology), phosphorylated Stat5 (Tyr694, D47E7, Cell Signaling Technology), Stat5 (Cell Signaling Technology), FLAG (M2, Sigma-Aldrich), Myc (Sigma-Aldrich), horseradish peroxidase (HRP)-conjugated light-chain-specific secondary antibodies (Abcam), and HRP-conjugated secondary antibodies (Santa Cruz Biotechnology). The rabbit polyclonal antibody against PTPN9 has been described previously (Su et al., 2012).

Statistical analysis

All experiments were repeated at least three times. A Student's *t*-test was performed to evaluate the significance of differences between experimental and control groups. $P < 0.05$ indicates a statistically significant effect.

Acknowledgements

We thank Zhizhuang J. Zhao (University of Oklahoma, Oklahoma City, OK), Qing-Yuan Sun (Institute of Zoology, Beijing, China), Feng Liu (Institute of Zoology, Beijing, China) and Iain C. Bruce (Zhejiang University, Hangzhou, China) for critical comments and reading of the manuscript; and members of Jing-Wei Xiong's laboratory for helpful discussion and technical assistance.

Competing interests

The authors declare no competing interests.

Author contributions

Y.B. designed and performed most of the experiments, and contributed to writing the manuscript; F.S. and Z.C. provided reagents and performed some of the biochemical experiments; X.W., H.G., L.L., N.C., Q.W., K.H. and X.Z. contributed some essential reagents and performed some zebrafish experiments; K.M.

conceived this work, designed experiments and analyzed data; J.-W.X. conceived this work, designed experiments, analyzed data and wrote the manuscript.

Funding

This work was supported by grants from the National Basic Research Program of China [grant numbers 2010CB529503 and 2012CB944501] and the National Science Foundation of China [grant numbers 31271549 and 31221002].

Supplementary material

Supplementary material available online at <http://jcs.biologists.org/lookup/suppl/doi:10.1242/jcs.145367/-DC1>

References

- Bertrand, J. Y., Kim, A. D., Teng, S. and Traver, D. (2008). CD41+ cmyb+ precursors colonize the zebrafish pronephros by a novel migration route to initiate adult hematopoiesis. *Development* **135**, 1853–1862.
- Chen, M. J., Yokomizo, T., Zeigler, B. M., Dzierzak, E. and Speck, N. A. (2009). Runx1 is required for the endothelial to haematopoietic cell transition but not thereafter. *Nature* **457**, 887–891.
- Cho, C. Y., Koo, S. H., Wang, Y., Callaway, S., Hedrick, S., Mak, P. A., Orth, A. P., Peters, E. C., Saez, E., Montminy, M. et al. (2006). Identification of the tyrosine phosphatase PTP-MEG2 as an antagonist of hepatic insulin signaling. *Cell Metab.* **3**, 367–378.
- Cooper, M. C., Levy, J., Cantor, L. N., Marks, P. A. and Rifkin, R. A. (1974). The effect of erythropoietin on colonial growth of erythroid precursor cells in vitro. *Proc. Natl. Acad. Sci. USA* **71**, 1677–1680.
- Cumano, A., Dieterlen-Lievre, F. and Godin, I. (1996). Lymphoid potential, probed before circulation in mouse, is restricted to caudal intraembryonic splanchnopleura. *Cell* **86**, 907–916.
- Danilova, N., Sakamoto, K. M. and Lin, S. (2011). Ribosomal protein L11 mutation in zebrafish leads to haematopoietic and metabolic defects. *Br. J. Haematol.* **152**, 217–228.
- de Jong, J. L. and Zon, L. I. (2005). Use of the zebrafish system to study primitive and definitive hematopoiesis. *Annu. Rev. Genet.* **39**, 481–501.
- Ezoe, S., Matsumura, I., Gale, K., Satoh, Y., Ishikawa, J., Mizuki, M., Takahashi, S., Minegishi, N., Nakajima, K., Yamamoto, M. et al. (2005). GATA transcription factors inhibit cytokine-dependent growth and survival of a hematopoietic cell line through the inhibition of STAT3 activity. *J. Biol. Chem.* **280**, 13163–13170.
- Foley, H. A., Ofori-Acquah, S. F., Yoshimura, A., Critz, S., Baliga, B. S. and Pace, B. S. (2002). Stat3 beta inhibits gamma-globin gene expression in erythroid cells. *J. Biol. Chem.* **277**, 16211–16219.
- Galloway, J. L., Wingert, R. A., Thisse, C., Thisse, B. and Zon, L. I. (2005). Loss of gata1 but not gata2 converts erythropoiesis to myelopoiesis in zebrafish embryos. *Dev. Cell* **8**, 109–116.
- Gering, M., Yamada, Y., Rabbitts, T. H. and Patient, R. K. (2003). Lmo2 and Scf/Tal1 convert non-axial mesoderm into haemangioblasts which differentiate into endothelial cells in the absence of Gata1. *Development* **130**, 6187–6199.
- Hall, C., Flores, M. V., Storm, T., Crosier, K. and Crosier, P. (2007). The zebrafish lysozyme C promoter drives myeloid-specific expression in transgenic fish. *BMC Dev. Biol.* **7**, 42.
- Hao, Q., Samten, B., Ji, H. L., Zhao, Z. J. and Tang, H. (2012). Tyrosine phosphatase PTP-MEG2 negatively regulates vascular endothelial growth factor receptor signaling and function in endothelial cells. *Am. J. Physiol.* **303**, C548–C553.
- Hu, K., Nan, X., Bird, A. and Wang, W. (2006). Testing for association between MeCP2 and the brahma-associated SWI/SNF chromatin-remodeling complex. *Nat. Genet.* **38**, 962–964, author reply 964–967.
- Huang, X., Gschweng, E., Van Handel, B., Cheng, D., Mikkola, H. K. and Witte, O. N. (2011). Regulated expression of microRNAs-126/126* inhibits erythropoiesis from human embryonic stem cells. *Blood* **117**, 2157–2165.
- Huynh, H., Bottini, N., Williams, S., Cherepanov, V., Musumeci, L., Saito, K., Bruckner, S., Vachon, E., Wang, X., Kruger, J. et al. (2004). Control of vesicle fusion by a tyrosine phosphatase. *Nat. Cell Biol.* **6**, 831–839.
- Jenkins, B. J., Quilici, C., Roberts, A. W., Grail, D., Dunn, A. R. and Ernst, M. (2002). Hematopoietic abnormalities in mice deficient in gp130-mediated STAT signaling. *Exp. Hematol.* **30**, 1248–1256.
- Jenkins, B. J., Roberts, A. W., Najdovska, M., Grail, D. and Ernst, M. (2005). The threshold of gp130-dependent STAT3 signaling is critical for normal regulation of hematopoiesis. *Blood* **105**, 3512–3520.
- Jopling, C., van Geemen, D. and den Hertog, J. (2007). Shp2 knockdown and Noonan/LEOPARD mutant Shp2-induced gastrulation defects. *PLoS Genet.* **3**, e225.
- Kalev-Zylinska, M. L., Horsfield, J. A., Flores, M. V., Postlethwait, J. H., Vitas, M. R., Baas, A. M., Crosier, P. S. and Crosier, K. E. (2002). Runx1 is required for zebrafish blood and vessel development and expression of a human RUNX1-CBF2T1 transgene advances a model for studies of leukemogenesis. *Development* **129**, 2015–2030.
- Kirito, K., Uchida, M., Takatoku, M., Nakajima, K., Hirano, T., Miura, Y. and Komatsu, N. (1998). A novel function of Stat1 and Stat3 proteins in erythropoietin-induced erythroid differentiation of a human leukemia cell line. *Blood* **92**, 462–471.

- Li, X., Xiong, J. W., Shelley, C. S., Park, H. and Arnaout, M. A. (2006). The transcription factor ZBP-89 controls generation of the hematopoietic lineage in zebrafish and mouse embryonic stem cells. *Development* **133**, 3641–3650.
- Lin, H. F., Traver, D., Zhu, H., Dooley, K., Paw, B. H., Zon, L. I. and Handin, R. I. (2005). Analysis of thrombocyte development in CD41-GFP transgenic zebrafish. *Blood* **106**, 3803–3810.
- Liu, F., Walmsley, M., Rodaway, A. and Patient, R. (2008). Fli1 acts at the top of the transcriptional network driving blood and endothelial development. *Curr. Biol.* **18**, 1234–1240.
- Ma, A. C., Ward, A. C., Liang, R. and Leung, A. Y. (2007). The role of jak2a in zebrafish hematopoiesis. *Blood* **110**, 1824–1830.
- Mantel, C., Messina-Graham, S., Moh, A., Cooper, S., Hangoc, G., Fu, X. Y. and Broxmeyer, H. E. (2012). Mouse hematopoietic cell-targeted STAT3 deletion: stem/progenitor cell defects, mitochondrial dysfunction, ROS overproduction, and a rapid aging-like phenotype. *Blood* **120**, 2589–2599.
- Minoo, P., Zadeh, M. M., Rottapel, R., Lebrun, J. J. and Ali, S. (2004). A novel SHP-1/Grb2-dependent mechanism of negative regulation of cytokine-receptor signaling: contribution of SHP-1 C-terminal tyrosines in cytokine signaling. *Blood* **103**, 1398–1407.
- Mucenski, M. L., McLain, K., Kier, A. B., Swerdlow, S. H., Schreiner, C. M., Miller, T. A., Pietryga, D. W., Scott, W. J., Jr and Potter, S. S. (1991). A functional c-myc gene is required for normal murine fetal hepatic hematopoiesis. *Cell* **65**, 677–689.
- Müller, A. M., Medvinsky, A., Strouboulis, J., Grosveld, F. and Dzierzak, E. (1994). Development of hematopoietic stem cell activity in the mouse embryo. *Immunity* **1**, 291–301.
- North, T. E., Goessling, W., Walkley, C. R., Lengerke, C., Kopani, K. R., Lord, A. M., Weber, G. J., Bowman, T. V., Jang, I. H., Grosser, T. et al. (2007). Prostaglandin E2 regulates vertebrate haematopoietic stem cell homeostasis. *Nature* **447**, 1007–1011.
- Ohneda, K., Ohmori, S., Ishijima, Y., Nakano, M. and Yamamoto, M. (2009). Characterization of a functional ZBP-89 binding site that mediates Gata1 gene expression during hematopoietic development. *J. Biol. Chem.* **284**, 30187–30199.
- Okuda, T., van Deursen, J., Hiebert, S. W., Grosveld, G. and Downing, J. R. (1996). AML1, the target of multiple chromosomal translocations in human leukemia, is essential for normal fetal liver hematopoiesis. *Cell* **84**, 321–330.
- Orkin, S. H. and Zon, L. I. (2008). Hematopoiesis: an evolving paradigm for stem cell biology. *Cell* **132**, 631–644.
- Paffett-Lugassy, N., Hsia, N., Fraenkel, P. G., Paw, B., Leshinsky, I., Barut, B., Bahary, N., Caro, J., Handin, R. and Zon, L. I. (2007). Functional conservation of erythropoietin signaling in zebrafish. *Blood* **110**, 2718–2726.
- Paik, E. J. and Zon, L. I. (2010). Hematopoietic development in the zebrafish. *Int. J. Dev. Biol.* **54**, 1127–1137.
- Pevny, L., Simon, M. C., Robertson, E., Klein, W. H., Tsai, S. F., D'Agati, V., Orkin, S. H. and Costantini, F. (1991). Erythroid differentiation in chimeric mice blocked by a targeted mutation in the gene for transcription factor GATA-1. *Nature* **349**, 257–260.
- Renshaw, S. A., Loynes, C. A., Trushell, D. M., Elworthy, S., Ingham, P. W. and Whyte, M. K. (2006). A transgenic zebrafish model of neutrophilic inflammation. *Blood* **108**, 3976–3978.
- Rhodes, J., Hagen, A., Hsu, K., Deng, M., Liu, T. X., Look, A. T. and Kanki, J. P. (2005). Interplay of pu.1 and gata1 determines myelo-erythroid progenitor cell fate in zebrafish. *Dev. Cell* **8**, 97–108.
- Rong, Y., Cheng, L., Ning, H., Zou, J., Zhang, Y., Xu, F., Liu, L., Chang, Z. and Fu, X. Y. (2006). Wilms' tumor 1 and signal transducers and activators of transcription 3 synergistically promote cell proliferation: a possible mechanism in sporadic Wilms' tumor. *Cancer Res.* **66**, 8049–8057.
- Scott, E. W., Simon, M. C., Anastasi, J. and Singh, H. (1994). Requirement of transcription factor PU.1 in the development of multiple hematopoietic lineages. *Science* **265**, 1573–1577.
- Shivdasani, R. A., Mayer, E. L. and Orkin, S. H. (1995). Absence of blood formation in mice lacking the T-cell leukaemia oncogene tal-1/SCL. *Nature* **373**, 432–434.
- Stainier, D. Y., Weinstein, B. M., Detrich, H. W., 3rd, Zon, L. I. and Fishman, M. C. (1995). Cloche, an early acting zebrafish gene, is required by both the endothelial and hematopoietic lineages. *Development* **121**, 3141–3150.
- Stewart, R. A., Sanda, T., Widlund, H. R., Zhu, S., Swanson, K. D., Hurley, A. D., Bentires-Alj, M., Fisher, D. E., Kontaridis, M. I., Look, A. T. et al. (2010). Phosphatase-dependent and -independent functions of Shp2 in neural crest cells underlie LEOPARD syndrome pathogenesis. *Dev. Cell* **18**, 750–762.
- Su, F., Ren, F., Rong, Y., Wang, Y., Geng, Y., Wang, Y., Feng, M., Ju, Y., Li, Y., Zhao, Z. J. et al. (2012). Protein tyrosine phosphatase Meg2 dephosphorylates signal transducer and activator of transcription 3 and suppresses tumor growth in breast cancer. *Breast Cancer Res.* **14**, R38.
- Sugiyama, M., Sakaue-Sawano, A., Imura, T., Fukami, K., Kitaguchi, T., Kawakami, K., Okamoto, H., Higashijima, S. and Miyawaki, A. (2009). Illuminating cell-cycle progression in the developing zebrafish embryo. *Proc. Natl. Acad. Sci. USA* **106**, 20812–20817.
- Tauchi, T., Damen, J. E., Toyama, K., Feng, G. S., Broxmeyer, H. E. and Krystal, G. (1996). Tyrosine 425 within the activated erythropoietin receptor binds Syp, reduces the erythropoietin required for Syp tyrosine phosphorylation, and promotes mitogenesis. *Blood* **87**, 4495–4501.
- Tauchi, T., Feng, G. S., Marshall, M. S., Shen, R., Mantel, C., Pawson, T. and Broxmeyer, H. E. (1994). The ubiquitously expressed Syp phosphatase interacts with c-kit and Grb2 in hematopoietic cells. *J. Biol. Chem.* **269**, 25206–25211.
- Traver, D., Paw, B. H., Poss, K. D., Penberthy, W. T., Lin, S. and Zon, L. I. (2003). Transplantation and in vivo imaging of multilineage engraftment in zebrafish bloodless mutants. *Nat. Immunol.* **4**, 1238–1246.
- Valentino, L. and Pierre, J. (2006). JAK/STAT signal transduction: regulators and implication in hematological malignancies. *Biochem. Pharmacol.* **71**, 713–721.
- Warren, A. J., Colledge, W. H., Carlton, M. B., Evans, M. J., Smith, A. J. and Rabbitts, T. H. (1994). The oncogenic cysteine-rich LIM domain protein rbt2 is essential for erythroid development. *Cell* **78**, 45–57.
- Welte, T., Zhang, S. S., Wang, T., Zhang, Z., Hesslein, D. G., Yin, Z., Kano, A., Iwamoto, Y., Li, E., Craft, J. E. et al. (2003). STAT3 deletion during hematopoiesis causes Crohn's disease-like pathogenesis and lethality: a critical role of STAT3 in innate immunity. *Proc. Natl. Acad. Sci. USA* **100**, 1879–1884.
- Woo, A. J., Moran, T. B., Schindler, Y. L., Choe, S. K., Langer, N. B., Sullivan, M. R., Fujiwara, Y., Paw, B. H. and Cantor, A. B. (2008). Identification of ZBP-89 as a novel GATA-1-associated transcription factor involved in megakaryocytic and erythroid development. *Mol. Cell. Biol.* **28**, 2675–2689.
- Woo, A. J., Kim, J., Xu, J., Huang, H. and Cantor, A. B. (2011). Role of ZBP-89 in human globin gene regulation and erythroid differentiation. *Blood* **118**, 3684–3693.
- Xiao, W., Hong, H., Kawakami, Y., Kato, Y., Wu, D., Yasudo, H., Kimura, A., Kubagawa, H., Bertoli, L. F., Davis, R. S. et al. (2009). Tumor suppression by phospholipase C-β3 via SHP-1-mediated dephosphorylation of Stat5. *Cancer Cell* **16**, 161–171.
- Xiong, J. W., Yu, Q., Zhang, J. and Mably, J. D. (2008). An acyltransferase controls the generation of hematopoietic and endothelial lineages in zebrafish. *Circ. Res.* **102**, 1057–1064.
- Xu, M. J., Sui, X., Zhao, R., Dai, C., Krantz, S. B. and Zhao, Z. J. (2003). PTP-MEG2 is activated in polycythemia vera erythroid progenitor cells and is required for growth and expansion of erythroid cells. *Blood* **102**, 4354–4360.
- Yao, X., Kodeboyina, S., Liu, L., Dzandu, J., Sangerman, J., Ofori-Acquah, S. F. and Pace, B. S. (2009). Role of STAT3 and GATA-1 interactions in gamma-globin gene expression. *Exp. Hematol.* **37**, 889–900.
- Yuan, T., Wang, Y., Zhao, Z. J. and Gu, H. (2010). Protein-tyrosine phosphatase PTPN9 negatively regulates ErbB2 and epidermal growth factor receptor signaling in breast cancer cells. *J. Biol. Chem.* **285**, 14861–14870.
- Zakrzewska, A., Cui, C., Stockhammer, O. W., Benard, E. L., Spaink, H. P. and Meijer, A. H. (2010). Macrophage-specific gene functions in Spi1-directed innate immunity. *Blood* **116**, e1–e11.